Supplementary Information

Thioguanine-Coordinated Assembly for Synthetic Lethality of Colorectal Cancer with Defective Mismatch Repair

Xiang Xu[a], Zhou Yang[a], Zhiyuan Xu[a], Taikang Wu[a], Lina Wu*[b], and Jianping Lei*[a]

[a]*State Key Laboratory of Analytical Chemistry for Life Science, School of Chemistry and Chemical Engineering, Nanjing University, Nanjing, 210023, China*

[b]*State Key Laboratory of Microbial Technology, School of Food Science and Pharmaceutical Engineering, Nanjing Normal University, Nanjing, 210023, China*

Corresponding authors:

Prof. Jianping Lei, *E-mail:* jpl@nju.edu.cn (J. Lei)

Prof. Lina Wu, *E-mail*: wuln@njnu.edu.cn (L. Wu)

Keywords: coordination; chemotherapy; synthetic lethality; metal-organic polymers; defective mismatch repair

Supporting Methods

Materials and reagents. Thioguanine and acetic acid were purchased from Sigma-Aldrich (Merck, USA). Acetonitrile, polyethylene glycol, cupric nitrate, and ammomium fluosilicate were obtained from Sinopharm Chemical Reagent Co., Ltd. and used directly without further purification. The cell culture media (Dulbecco's Modified Eagle Medium, DMEM), Roswell Park Memorial Institute 1640 (RPMI-1640), trypsin-EDTA (ethylenediaminetetraacetic acid), and penicillin/streptomycin were from SenBeiJia Biological Technology Co., Ltd. (China). NSC (National Cancer Institute Diversity Set library) 19630 and iodine were purchased from Bidepharm. Cell Counting Kit-8 (CCK-8), EdU cell proliferation kit, rabbit polyclonal antibody (anti-PCNA, anti-PARP, anti-H2AX, anti-53BP1, anti-p-P53), and the Alexa Fluor 647-conjugated secondary antibody (anti-rabbit secondary antibody) were obtained from Beyotime Technology Co., Ltd. (China). Primers were purchased from Sangon Biotech (Shanghai) Co., Ltd. RNA reverse transcription kit and qPCR kit were purchased from Beijing Tsingke Biotech Co., Ltd. All aqueous solutions were prepared using ultrapure water (≥ 18 MΩ·cm, Milli-Q, Millipore).

Characterizations. The scanning electron microscope (SEM) images were recorded on a JSM-7800F high resolution scanning electron microscope (JEOL Ltd., Japan). The transmission electron microscopic (TEM) images were recorded on a JEM-2100 high resolution transmission electron microscope (JEOL Ltd., Japan). The zeta potential was measured on Nano-Z Zetasizer (Malvern Panalytical, UK). Powder X-ray diffraction (PXRD) data was obtained by a X'TRA diffractometer (ARL, Switzerland). The ultraviolet absorption spectra were obtained with a UV-3600 UV-Vis-NIR spectrophotometer (Shimadzu Co., Japan). CCK-8 assays were carried out on a Synergy hybrid 1 multimode microplate reader (BioTek). The cell images were gained on a TCS SP8 laser scanning confocal microscope (Leica, Germany). Flow cytometric analysis was performed on a Coulter FC-500 flow cytometer (Beckman-Coulter). High resolution mass data were run on an Agilent 6530 TOF LC/MS mass spectrometer.

Synthesis of TGSSTG. TGSSTG was synthesized according to previous report with little modification. Briefly, 1.4 g 6-TG was dispersed in 300 mL of saturated sodium bicarbonate solution under heating, then the mixture was allowed cooled to room temperature. After that, 2.1 g I_2 was dissolved in 8 mL DMF and dropped into abovementioned mixture dropwise. The system was further stirred 4 h and the sediment was collected by centrifugation. The sediment was washed with water several times and dried under vacuum.

Synthesis of MOP, MN, and MNP.

MOP: Briefly, 20 mg TGSSTG was dispersed in 1.5 mL acetonitrile, then $Cu(NO_3)_2 \cdot 3H_2O$ (7.2 mg) and $(NH_4)_2SiF_6$ (5.4 mg) dissolved in 0.5 mL of distilled water were added. The mixture was stirred at 58 °C for 12 h to yield a powder product in water bath. The products were separated via centrifugation at 9,000 rpm for 2 min and washed with acetonitrile for several times to remove impurities as much as possible. Finally, the product was dried at 50 °C under vacuum (with a mass of around 22 mg). For synthesis of nanoscaled **MOP**, 1.0 mL acetic acid was extra added.

MN: 1.0 mg **MOP** was dispersed in 1.0 mL of distilled water, then 2.0 mg NSC 19630 was added. After 12 h stirring, the product was harvested by centrifugation and washed several times with water. Finally, the product was dried at 50 °C under vacuum. The remaining NSC 19630 was quantified by the characteristic absorbance of NSC 19630 at 218 nm according to the standard curve between UV absorbance vs NSC 19630 concentrations. Finally, the loading efficiency was determined to be 22%.

MNP: 1.0 mg **MN** was dispersed in 1.0 mL of methanol, and 10 mg polyethylene glycol dissolved in chloroform was added. The mixture was stirred for 12 h at room temperature. The resulting product was harvested by centrifugation and washed several times with water, resulting in production of **MNP**.

GSH-responsive drug release. MNP was dispersed in PBS containing 10 m GSH at a concentration of 40 μg mL^{-1}, the mixture was stirred for 4 h, followed by centrifugation. Liquid supernatant was

submitted to liquid chromatograph mass spectrometer (LC-MS) analysis, pure thioguanine was analyzed as control.

Cell culture. Human colorectal cancer cancer cell lines (SW480, SW620, HCT15, and HCT116) were provided by the Institute of Basic Medical Sciences, Chinese Academy of Medical Sciences. SW480 and SW620 were cultured in RPMI-1640 while HCT15, and HCT116 were cultured in DMEM supplemented with 10% (v/v) fetal bovine serum (FBS), penicillin (100 U mL^{-1}) and streptomycin (100 μg mL^{-1}) at 37°C in a humidified incubator under 5% CO_2. The cells were routinely harvested by the use of a trypsin-EDTA solute on (0.25%) until the confluence was reached.

In vitro cytotoxicity assay. *In vitro* cytotoxicity was assessed by the standard cell counting kit-8 (CCK-8) assay. Firstly, SW480, SW620, HCT15, and HCT116 cells were seeded in 96 well-plates at a density of 5 $\times 10^3$ cells per well for 24 h. Then the cells were incubated with different concentration of PBS or **MNP**. After the cells were further incubated for 24 h, the medium was removed. Then, 100 μL of fresh medium with 10 μL of CCK-8 solution was added and incubated for another 1 h. The absorbance at 450 nm was measured to calculate the cell viability by a microplate reader. The statistical evaluation of data was performed using a two-tailed unpaired Student's t-test. Each data point is represented as mean ± standard deviation (SD) of independent experiments (n = 6, n indicates the number of wells in a plate for each experimental condition).

Clonogenic assay. SW480, SW620, HCT15, and HCT116 cells were seeded in 12-well plates at a density of 5 $\times 10^3$ cells per well for 24 h. After 24 h of incubation with **MNP**, cells were subsequently propagated for 7 days in **MNP**-free medium, which was changed every 3 days. Then cells were stained with crystal violet. Briefly, cells were fixed with 10% formalin for 30 min at room temperature, followed with staining by 0.1% crystal violet in 70% ethanol (250 μL per well) for 30 min. Next, cells were washed with deionized water three times for 5 min each to remove unbounded crystal violet. Finally, crystal violet dye was extracted with 250 μL of 10% acetic acid. Then, 50 μL the above solution was transferred into a 96-well format in triplicate for quantitation.

Cell proliferation assay. SW480, SW620, HCT15, and HCT116 cells were seeded in 35-mm confocal dish at the density of 1×10^4 cells per well. After adherent, the cells were cultured with PBS, or **MNP** for 24 h, then cells were washed with PBS several times and cultured with fresh medium. EdU (10 μM) was added to the culture medium, and cells were incubated at 37 °C for 2 h. Cells were washed with PBS and fixed with 3.7% formaldehyde at room temperature for 20 min. Following fixation, cells were washed with washing buffer three times (5 min each time) and incubated with permeabilization buffer for 30min. After permeabilization, cells were washed three times (5 min each time) with washing buffer, then 0.5 mL Click-iT reaction mixture (1× Click-iT reaction buffer, $CuSO_4$, Alexa Fluor 594 Azide, and reaction buffer additive) (Beyotime) was added to each well and cells were incubated at room temperature for 30 min in the dark. Cells were washed three times (5 min each time) with washing buffer and incubated with DAPI (0.5 μg mL^{-1} in PBS), then cells were washed with washing buffer and soaked in 3.7% formaldehyde. The confocal laser scanning microscope (CLSM) images were collected at 420-500 nm under the 405 nm excitation for DAPI channel, and 610-620 nm under the 590 nm excitation for Alexa Fluor 594 Azide channel.

Flow cytometry analysis of apoptosis. SW480, SW620, HCT15, and HCT116 cells were seeded 6-well plates at a density of 1×10^5 cells per well for 24 h. After adherent, cells were cultured with PBS, or **MNP** for 24 h, the culture medium was centrifuged to harvest apoptotic cells. Then, cells on plates were washed twice and detached by trypsinization. Cells were washed twice with PBS and stained with FITC-Annexin V and PI for 10 minutes. The cells were tested with flow cytometry.

Immunofluorescence. SW480, SW620, HCT15, and HCT116 cells were seeded in 35-mm confocal dish at the density of 1×10^4 cells per well. After adherent, the cells were cultured with PBS, or **MNP** for 24 h, then cells were washed with PBS several times and fixed with 3.7% formaldehyde at room temperature for 20 min. Following fixation, cells were washed with washing buffer three times (5 min each time) and incubated with permeabilization buffer for 30 min. After permeabilization, cells were washed three times (5 min each time) with washing buffer, followed by incubated with blocking buffer for 1 h. Cells were washed three times (5 min each time) with

washing buffer. Then primary antibody diluted at a ratio of 1:200 (PCNA, PARP H2AX, 53BP1, p-P53) (Beyotime) was added to each well and cells were incubated at 4 °C for overnight. After washed three times (5 min each time) with washing buffer, cells were incubated with secondary antibody conjugated with Alexa Fluor 647 for 2 h. Then cells were washed three times (5 min each time) with washing buffer and incubated with DAPI (0.5 μg mL^{-1} in PBS). After washed with washing buffer, cells were soaked in 3.7% formaldehyde. The CLSM images were collected at 420-500 nm under the 405 nm excitation for DAPI channel, and 660-675 nm under the 651 nm excitation for Alexa Fluor 647 channel.

Flow cytometry analysis of cell cycle. SW480, SW620, HCT15, and HCT116 cells were seeded 6-well plates at a density of 1 $\times 10^5$ cells per well for 24 h. After adherent, cells were cultured with PBS, or **MNP** for 24 h. Then, cells were washed twice with PBS and detached by trypsinization. Cells were harvested and washed twice with cold PBS. After soaked in cold 70% ethanol for 4 h, cells were washed twice with PBS followed by incubated with RNase A and PI for 1 h. Then, the cells were tested with flow cytometry and cell cycle was determined by the contents of DNA.

Quantification of cyclin E1, p21, and chk 1. SW480, SW620, HCT15, HCT116 cells were seeded 6-well plates at a density of 1 $\times 10^5$ cells per well for 24 h. After adherent, cells were cultured with PBS, or **MNP** for 24 h. Then, cells were washed twice and detached by trypsinization. Total RNA was extracted using a RNA extraction kit, and reversed to cDNA. Then the cDNA was used for qPCR, GAPDH was set as the reference gene. Primers were list as follows: cyclin E1-F, TGTGTCCTGGATGTTGACTGCC; cyclin E1-R, CTCTATGTCGCACCACTGATACC; p21-F, AGGTGGACCTGGAGACTCTCAG; p21-R, GATGCTTCCCAGAAATCCCCC; chk1-F, GTGTCAGAGTCTCCCAGTGGAT; chk1-R, GTTCTGGCTGAGAACTGGAGTAC; GAPDH-F, GCCTCAAGATCATCAGCAAT; GAPDH-R, TTCAGCTCAGGGATGACCTT.

Therapeutic treatments in vivo. All animal assays obeyed the institutional animal use and care regulations approved by the Model Animal Research Center of Nanjing University (MARC). To

establish the tumor bearing xenograft mouse model, female BALB/c mice (6-8 weeks-old) were chosen to be inoculated with SW480, SW620, HCT15, HCT116 cells (1.0×10^6) subcutaneously into the right flank position. Tumor sizes were measured using a digital caliper. The tumor volumes were calculated using formula $V = 0.5 \times A \times B^2$ (A refers to the tumor length and B refers to the tumor width). After the tumor volume of mice approached about 100 mm^3, these mice were randomly grouped and injected with PBS or **MNP**. Then, the tumor-bearing mice (n = 4 mice per group) were intratumorly injected with a formulation of 1 mg/kg every other day. All injections were administered in total, at 2-day intervals. Tumor volumes were measured every day for 14 days. Finally, the mice were humanely killed and the tumors were harvested after 14 d of treatment.

H&E staining and immunohistochemical staining. The mice were killed after 14 d of treatment, and representative heart, liver, spleen, lung, kidney, and tumor tissues were collected for histology analysis. The tissues were sliced and dehydrated, dehydration and stained with haematoxylin and eosin (H&E). The H&E staining images were observed under the brightfield microscopy (Olympus, Japan). For immunohistochemistry assays, tumors slices were treated for immunohistochemistry, according to the manufacturer's instructions.

Supplementary Figures

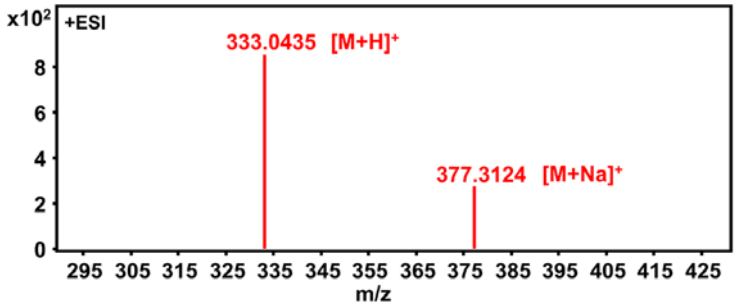

Fig. S1. Mass spectrum analysis of TGSSTG. HRESIMS m/z 333.0435 $[M+H]^+$ (calcd for $C_{10}H_9N_{10}S_2$, 333.0448).

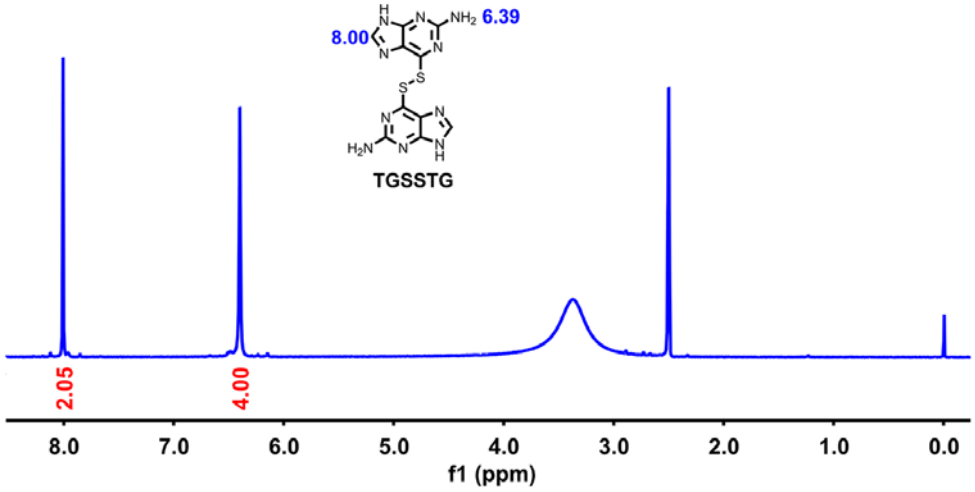

Fig. S2. ^{1}H NMR spectrum of TGSSTG in DMSO-d_6 at 400 MHz.

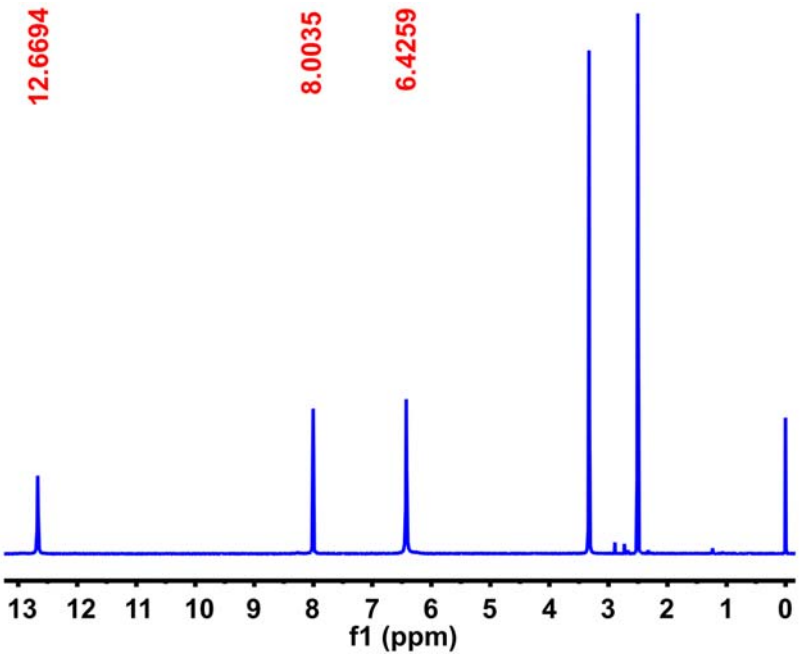

Fig. S3. ^{1}H NMR spectrum of TGSSTG stored at room temperature for over six months. Analyzed in DMSO-d_6 at 400 MHz.

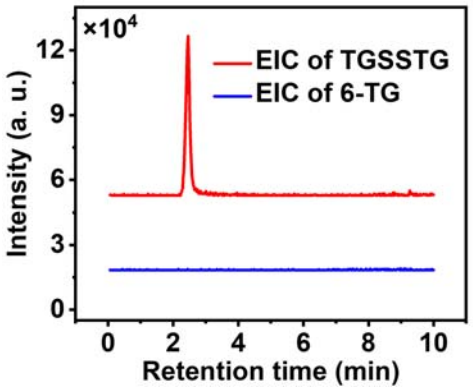

Fig. S4. Extracted ion chromatogram (EIC) of the mass spectrum of synthesized TGSSTG.

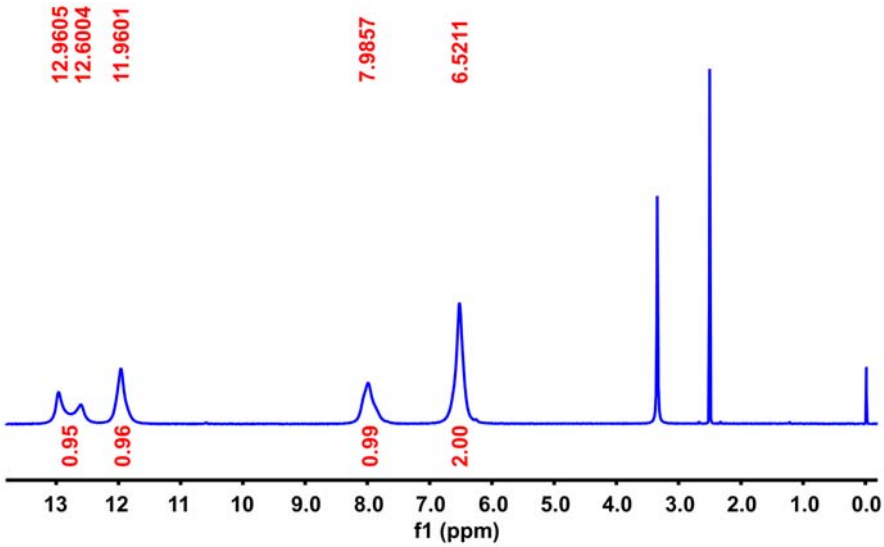

Fig. S5. ^{1}H NMR spectrum of 6-TG in DMSO-d_6 at 400 MHz.

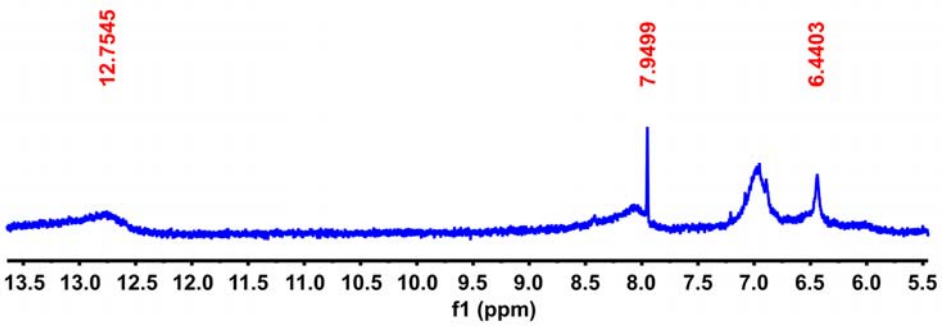

Fig. S6. ^{1}H NMR spectrum of the disassembly product of MOPs. Analyzed in DMSO-d_6 at 400 MHz.

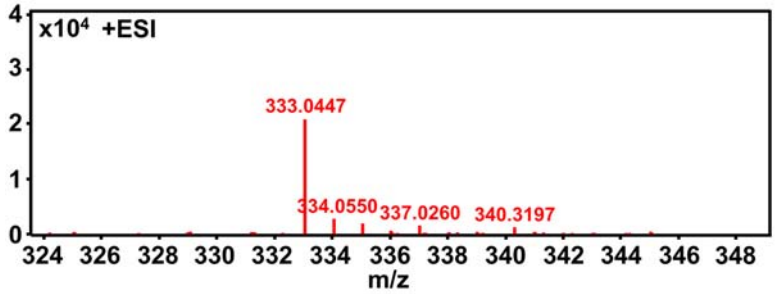

Fig. S7. Mass spectrum of the disassembly product of MOPs. HRESIMS m/z 333.0447 $[M+H]^+$ (calcd for $C_{10}H_9N_{10}S_2$, 333.0448).

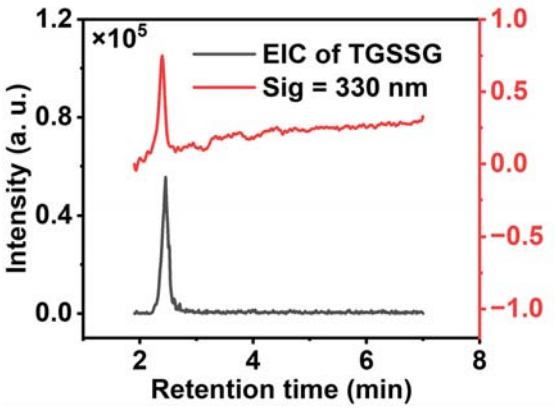

Fig. S8. LC-MS analysis of the disassembly product of MOPs.

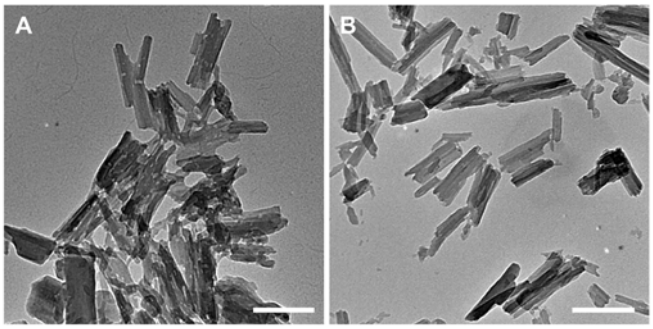

Fig. S9. TEM images of (**A**) **M** and (**B**) **MN**, scale bars = 200 nm.

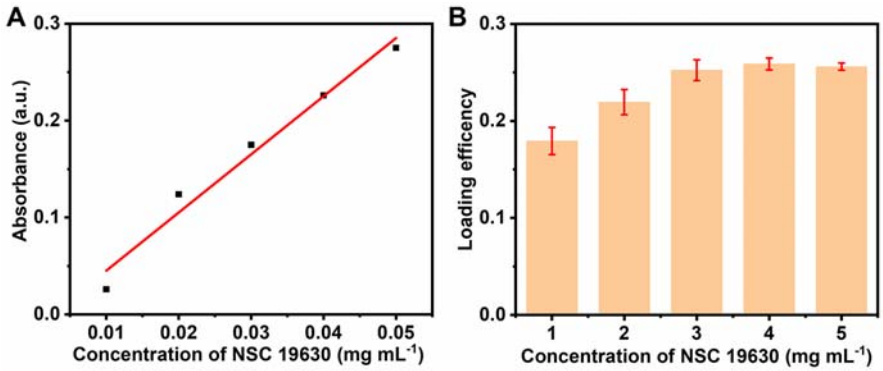

Fig. S10. (**A**) Standard curve of absorbance of ultraviolet vs NSC 19630 concentrations. (**B**) The loading efficiency of NSC 19630 under different concentrations.

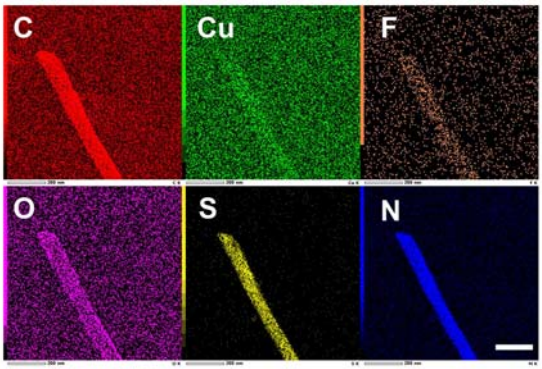

Fig. S11. Elemental mapping of **MNP** by TEM (scale bar = 200 nm).

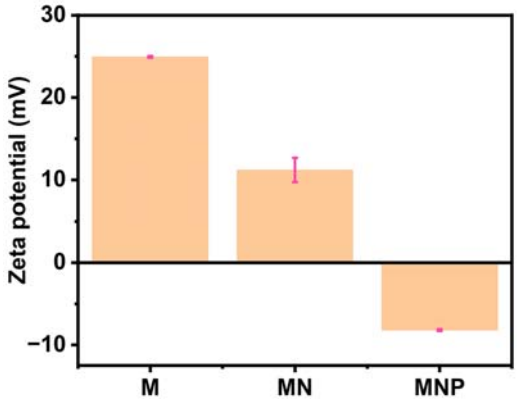

Fig. S12. Zeta potentials of **M**, **MN**, and **MNP**.

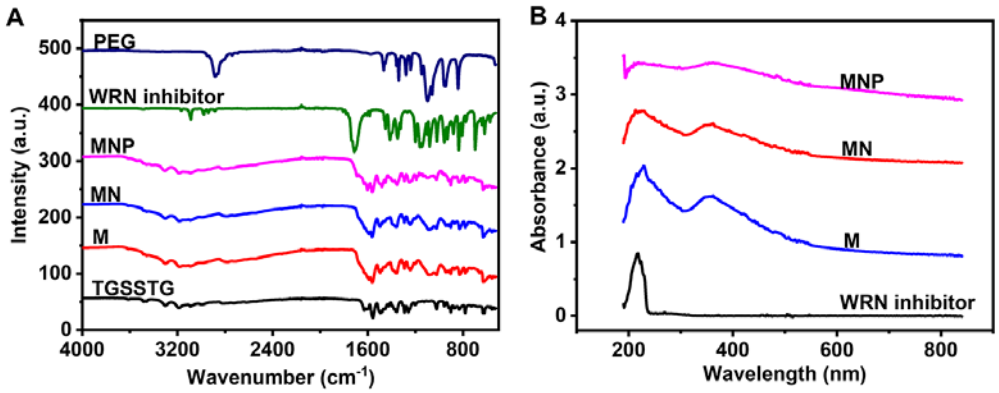

Fig. S13. The infrared (**A**) and (**B**) UV-vis spectra of **M**, NSC 19630, **MN**, and **MNP**.

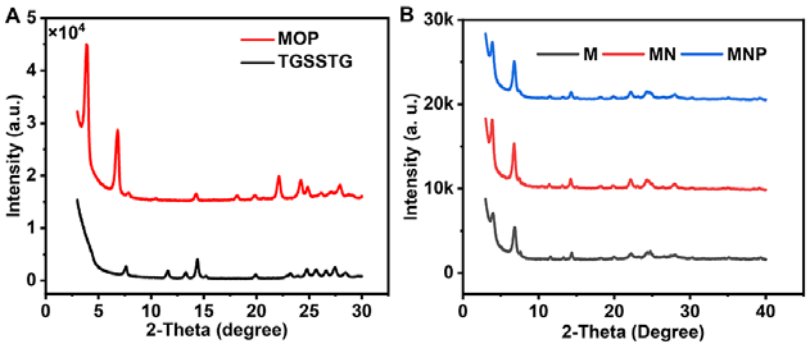

Fig. S14. (**A**) PXRD patterns of MOP and TGSSTG. (**B**) PXRD patterns of **M**, **MN**, and **MNP**.

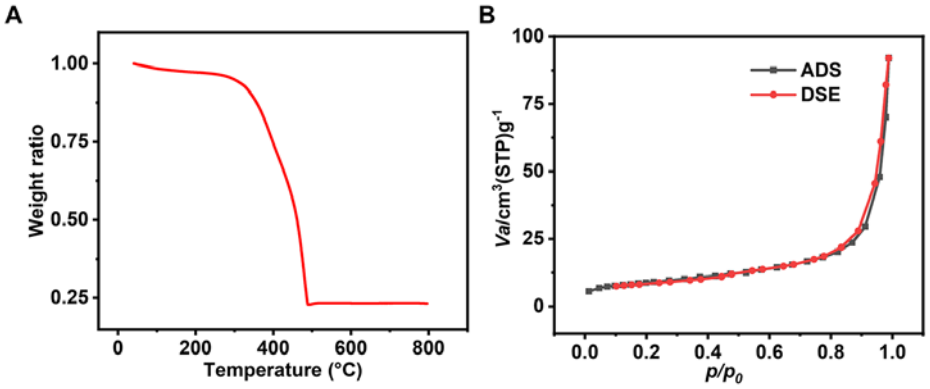

Fig. S15. (**A**) The thermogravimetry analysis in air atmosphere and (**B**) N_2 adsorption/desorption isotherms of **M**.

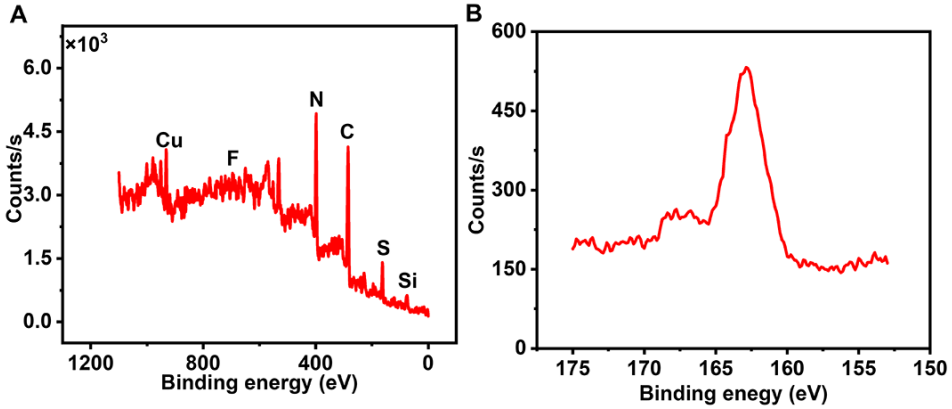

Fig. S16. (**A**) XPS survey spectrum of **M**. (**B**) XPS high-resolution spectrum of S 2p in **M**.

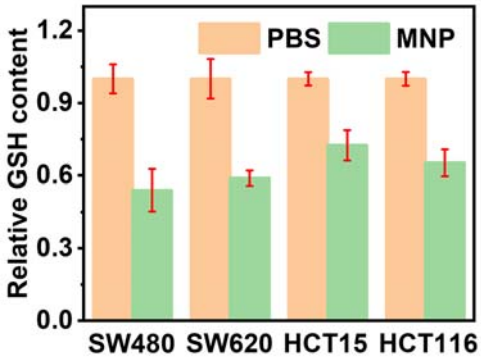

Fig. S17. Relative GSH content in PBS and **MNP**-treated cells.

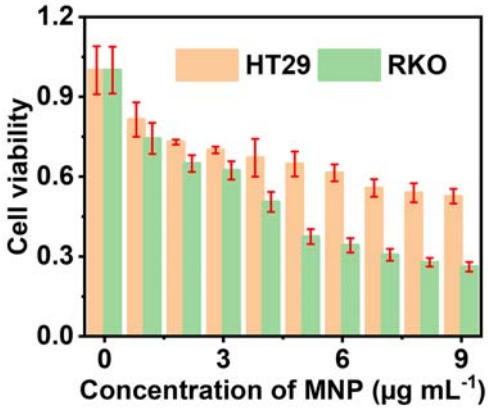

Fig. S18. Relative cell viabilities of HT29 (proficient MMR) and RKO (dMMR) cells treated with **MNP** at different concentrations.

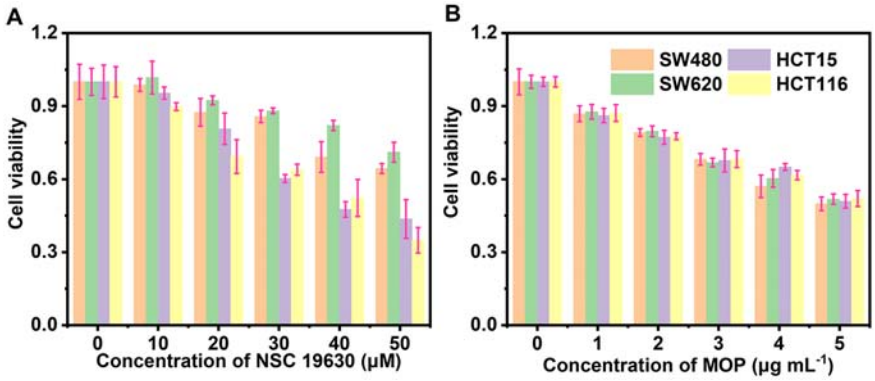

Fig. S19. Relative cell viabilities of cells treated with (**A**) NSC 19630 and (**B**) **M** at different concentrations.

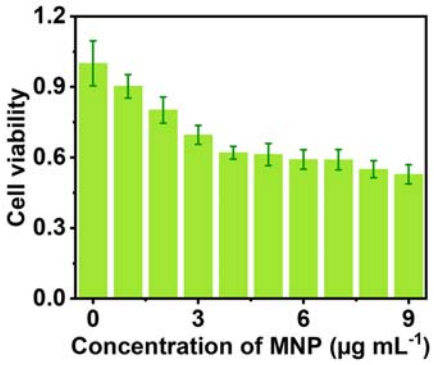

Fig. S20. Relative cell viabilities of MCF10A cells treated with **MNP** at different concentrations.

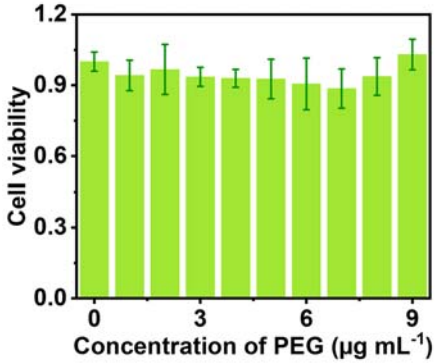

Fig. S21. Relative cell viabilities of SW480 cells treated with PEG at different concentrations.

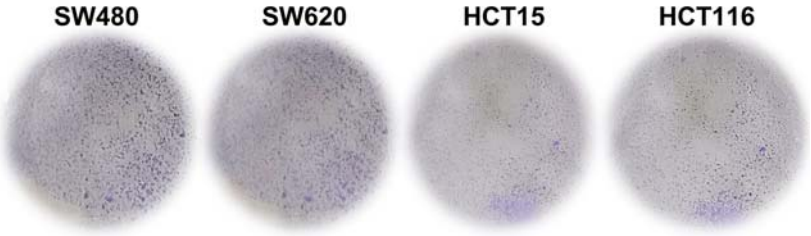

Fig. S22. Clonogenic assay of four cell lines after treated with 2.0 μg mL^{-1} **MNP**.

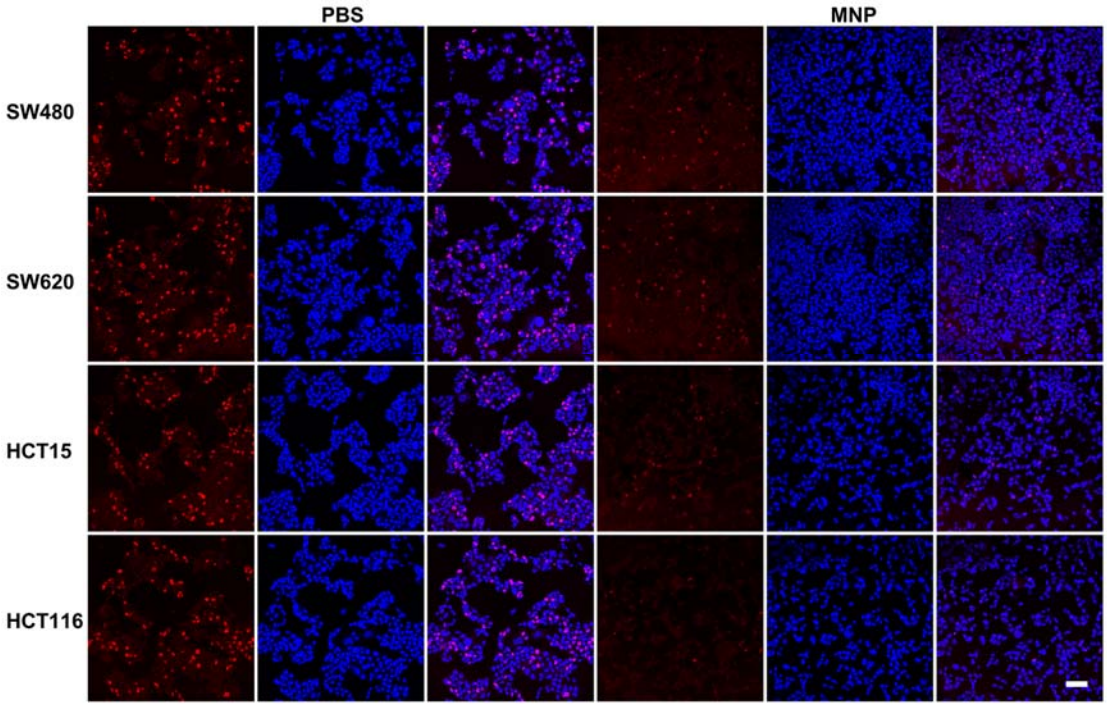

Fig. S23. CLSM images of cells stained with Hoechst 33342 and Alexa Fluor 594 Azide after treated with PBS and 2.0 μg mL^{-1} **MNP**. Scale bar = 75 μm.

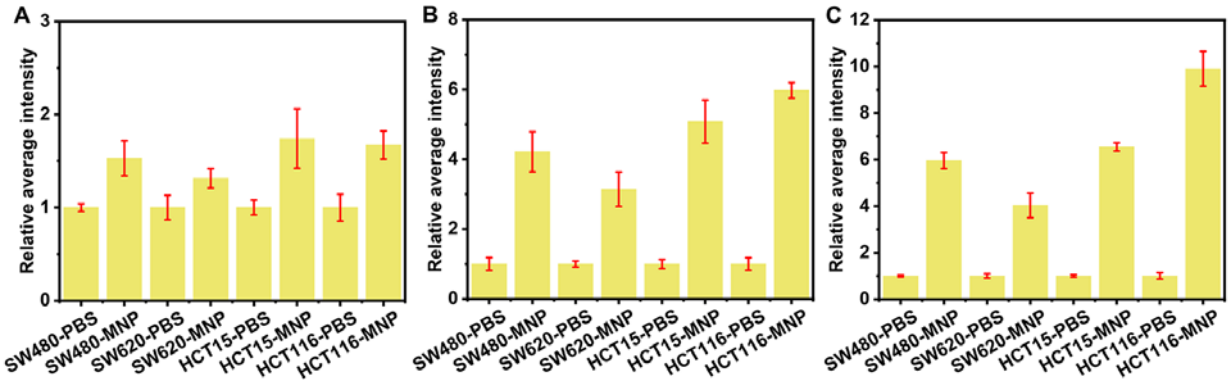

Fig. S24. Quantification of imaging data of (A) PCNA, (B) PARP, and (C) γH2AX, presented as means ± SD from three independent experiments.

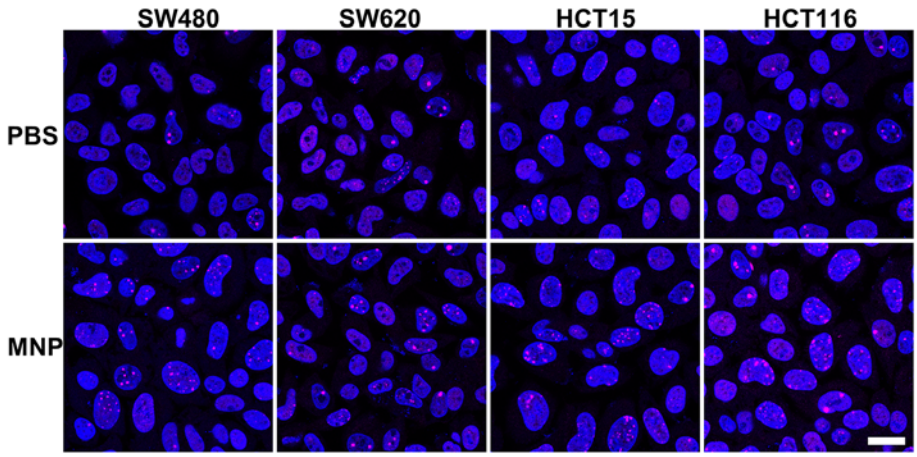

Fig. S25. CLSM images of immunofluorescence against 53BP1 after cells were treated with PBS and 2.0 μg mL^{-1} **MNP**, followed by incubation of 53BP1 primary antibody and Alexa Fluor 647-labeled secondary antibody. Hoechst staining was used to mark nuclei. Scale bar = 20 μm.

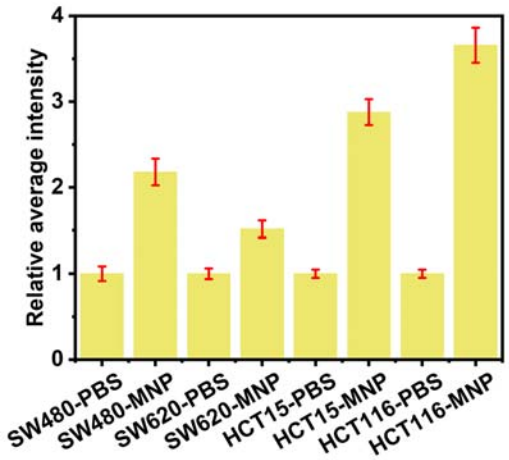

Fig. S26. Quantification of imaging data of 53BP1, presented as means ± SD from three independent experiments.

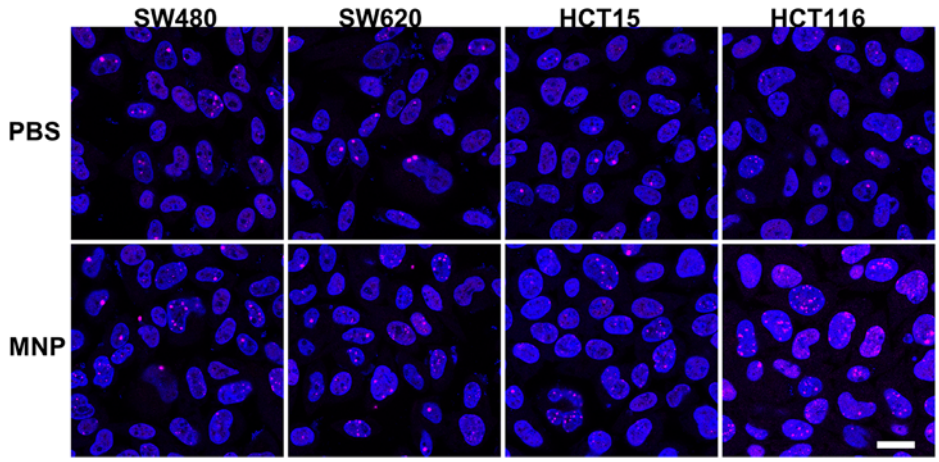

Fig. S27. CLSM images of immunofluorescence against phospho-p53 after cells were treated with PBS and 2.0 μg mL^{-1} **MNP**, followed by incubation of phospho-p53 primary antibody and Alexa Fluor 647-labeled secondary antibody. Hoechst staining was used to mark nuclei. Scale bar = 20 μm.

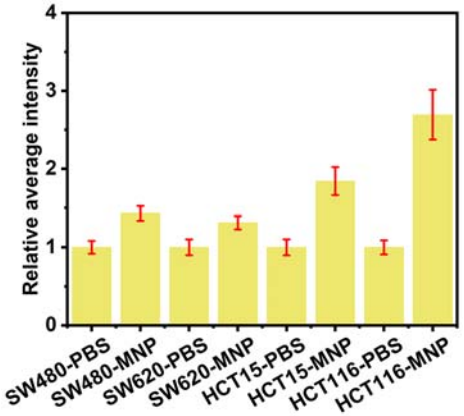

Fig. S28. Quantification of imaging data of phospho-p53, presented as means ± SD from three independent experiments.

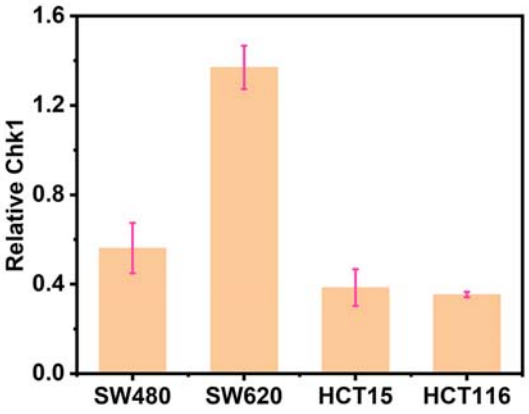

Fig. S29. Chk1 expression in four cell lines using GAPDH as the reference.

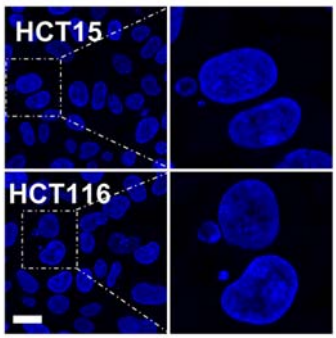

Fig. S30. Micronuclei in HCT15 and HCT116 after treated with PBS and 2 μg mL^{-1} **MNP**, scale bar = 20 μm.

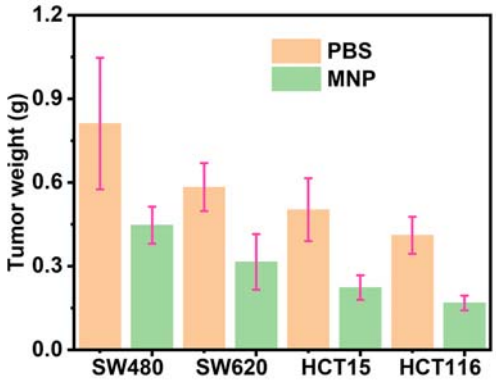

Fig. S31. Weight of extracted tumor after treated with PBS and **MNP**.

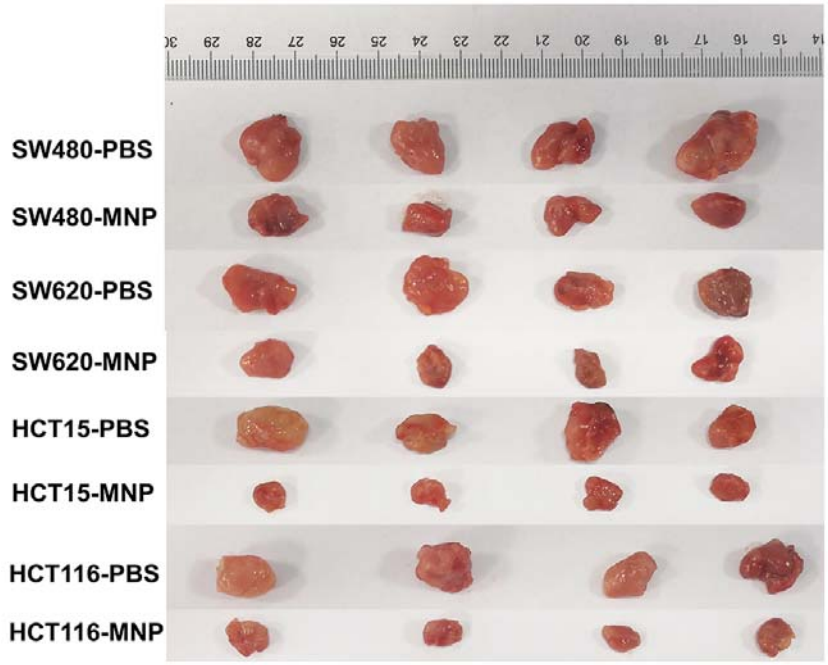

Fig. S32. Harvested tumors after mice were treated with PBS and **MNP** for 14 days.

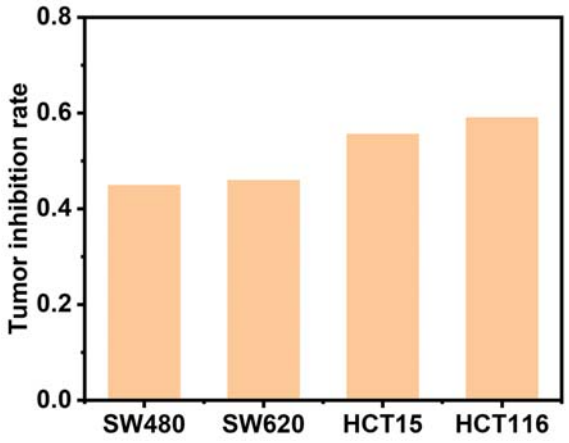

Fig. S33. Tumor inhibition rate of **MNP** towards four CRC tumor.

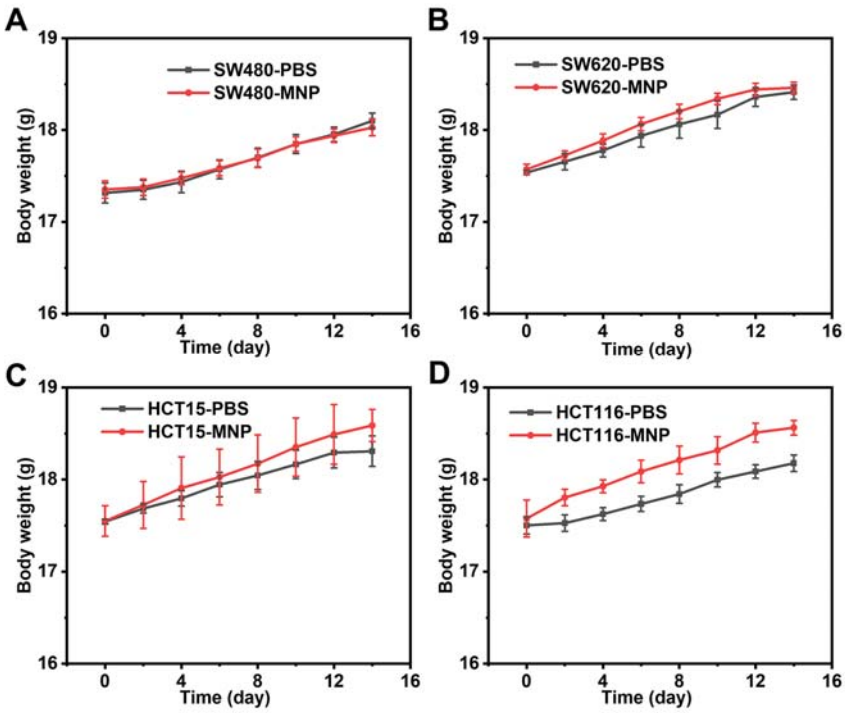

Fig. S34. Time-dependent body weight curves of nude mice bearing (**A**) SW480, (**B**) SW620, (**C**) HCT15, and (**D**) HCT116 tumors with PBS or **MNP** treatments in therapeutic progress.

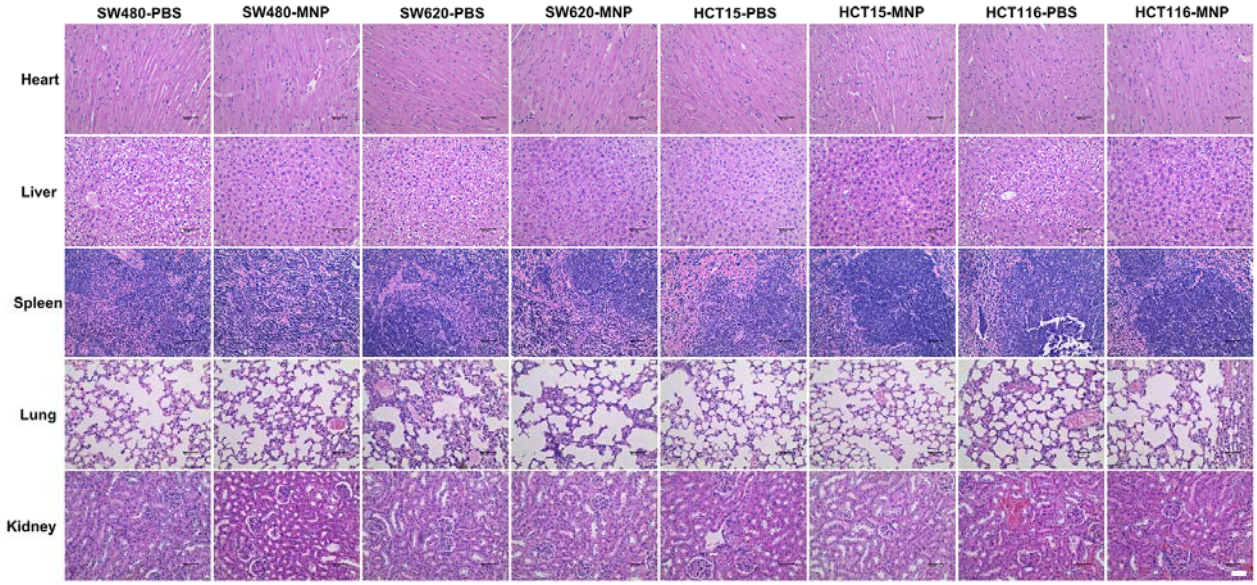

Fig. S35. H&E stained organ slices taken after 14 day-treatment (scale bar = 50 μm).

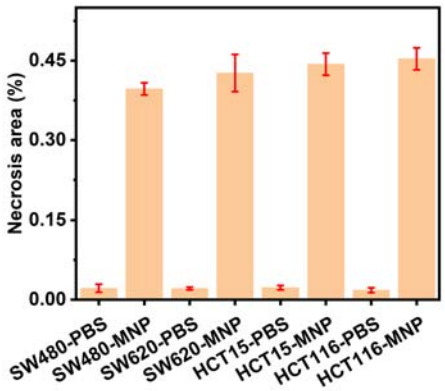

Fig. S36. Quantitative analyses of necrosis area. Data are presented as mean values ± SD (n = 3).

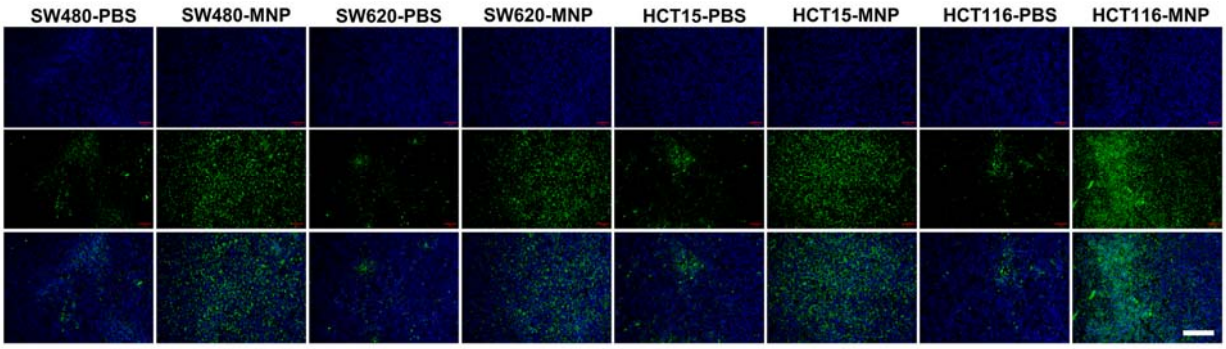

Fig. S37. CLSM images of immunofluorescence against cyt *c* of tumor tissues incubated with cyt *c* primary antibody and Alexa Fluor 647-labeled secondary antibody. Hoechst staining was used to mark nuclei. Scale bar = 50 μm.

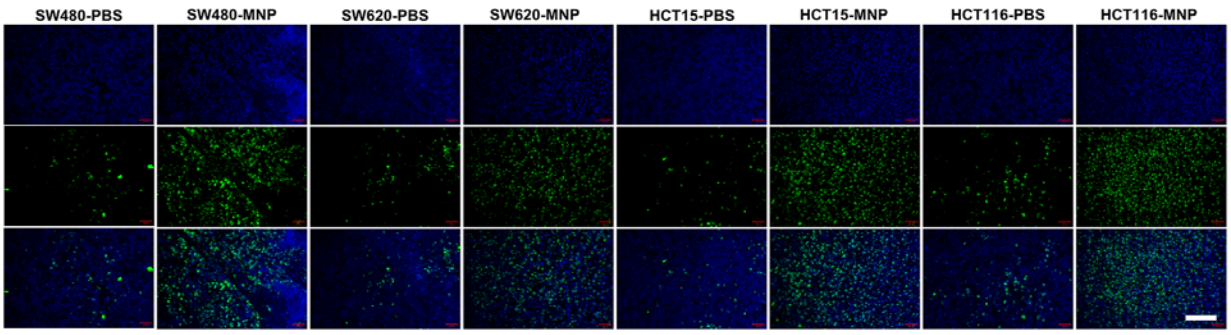

Fig. S38. CLSM images of immunofluorescence against PCNA of tumor tissues incubated with PCNA primary antibody and Alexa Fluor 647-labeled secondary antibody. Hoechst staining was used to mark nuclei. Scale bar = 50 μm.

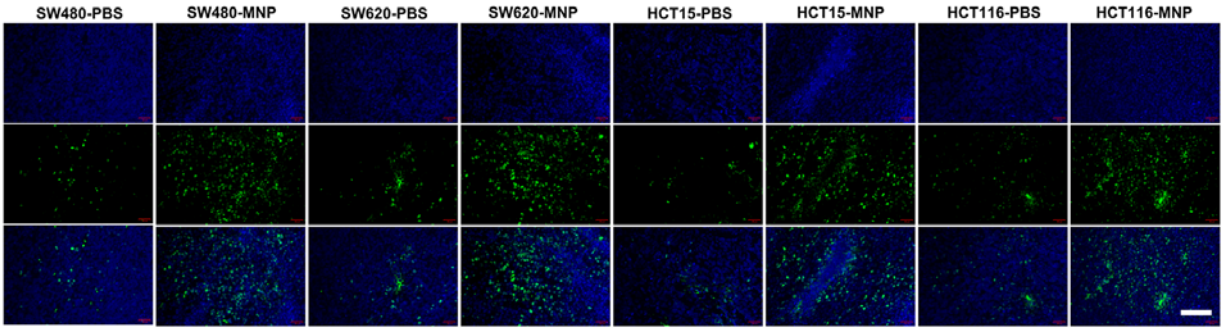

Fig. S39. CLSM images of immunofluorescence against PARP of tumor tissues incubated with PARP primary antibody and Alexa Fluor 647-labeled secondary antibody. Hoechst staining was used to mark nuclei. Scale bar = 50 μm.

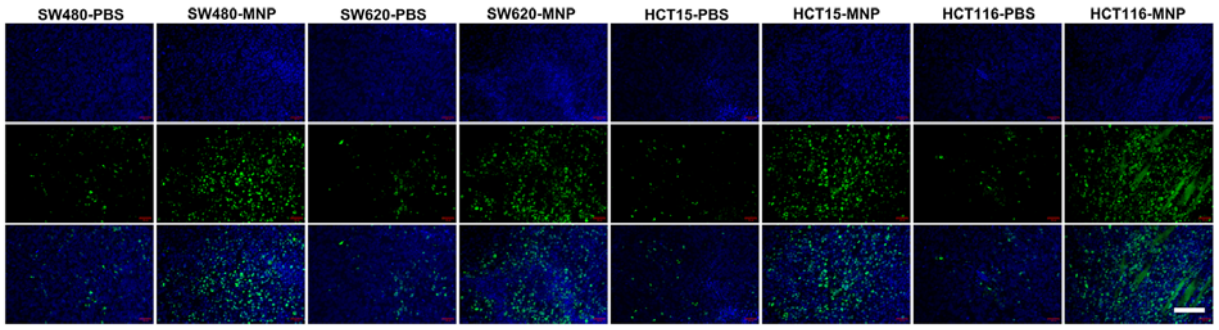

Fig. S40. CLSM images of immunofluorescence against γH2AX of tumor tissues incubated with γH2AX primary antibody and Alexa Fluor 647-labeled secondary antibody. Hoechst staining was used to mark nuclei. Scale bar = 50 μm.

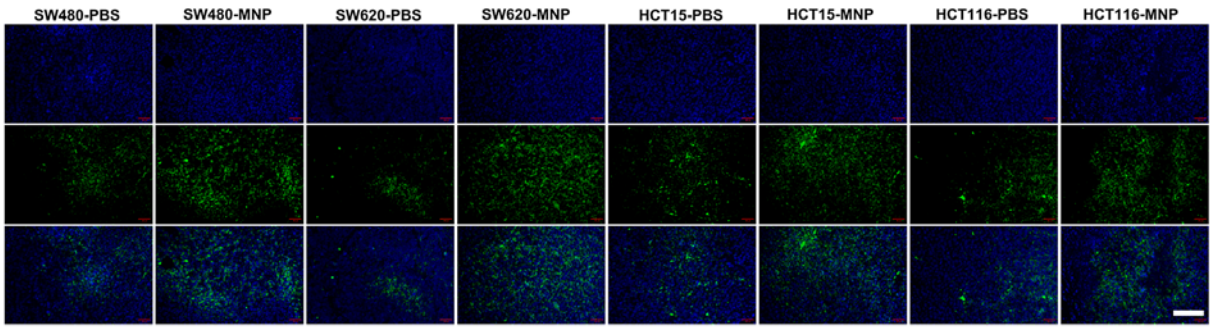

Fig. S41. CLSM images of immunofluorescence against 53BP1 of tumor tissues incubated with 53BP1 primary antibody and Alexa Fluor 647-labeled secondary antibody. Hoechst staining was used to mark nuclei. Scale bar = 50 μm.

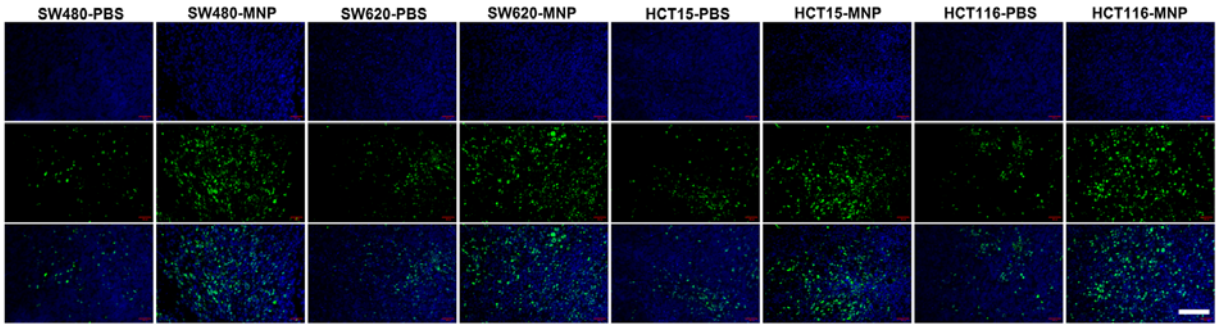

Fig. S42. CLSM images of immunofluorescence against phospho-p53 of tumor tissues incubated with phospho-p53 primary antibody and Alexa Fluor 647-labeled secondary antibody. Hoechst staining was used to mark nuclei. Scale bar = 50 μm.